



Dielectric response in the antiferromagnetic phase of $\text{Fe}_{1.10}\text{Te}$

Kazuoki Yokoi^a, Issei Miyazaki^a, Koichi Ichimura^{a,*}, Satoshi Tanda^a, Noriaki Matsunaga^b, Tohru Kurosawa^{b,1}, Migaku Oda^b

^a Department of Applied Physics, Hokkaido University, Sapporo, 060-8628, Japan

^b Department of Physics, Hokkaido University, Sapporo, 060-0810, Japan

ARTICLE INFO

Communicated by T. Kimura

Keywords:

Iron-based superconductor

Fe_{1+x}Te

STM

Dielectric response

Charge fluctuation

ABSTRACT

$\text{Fe}_{1.10}\text{Te}$ was studied by scanning tunneling microscopy (STM) and dielectric response to elucidate the charge fluctuation. The cleaved *a-b* surface was clearly imaged by UHV-STM at $T = 8.3$ K. From the line profiles, each Fe site was thought to be equivalent suggesting no static charge order in the antiferromagnetic phase. The temperature dependence of the dielectric permittivity was obtained by measuring the complex impedance. The dielectric permittivity increased with decreasing temperature below the Neel temperature T_N . The temperature dependence followed the Curie law, indicating the paraelectric state. It suggests charges fluctuate dynamically in the antiferromagnetic state. We conclude that the dynamical charge fluctuation cooperates with the antiferromagnetic order in $\text{Fe}_{1.10}\text{Te}$.

1. Introduction

Iron-based superconductors [1,2] have attracted much interest since the superconductivity occurs with highly correlated electrons such as high- T_c cuprates and organic superconductors [3]. A typical electronic phase diagram shows the competition between the superconducting state and the antiferromagnetic order [4]. Such a situation has been discussed by the Hubbard model [5–7] in which the transfer energy t and onsite Coulomb interaction U are taken into account. A higher U/t suppresses the superconductivity and causes the magnetic order. A charge stripe structure has been observed in high- T_c cuprates [8,9] and organic conductors [10]. According to the extended Hubbard model [11], such a charge ordered state is caused by the offsite Coulomb interaction V . The offsite (long range) Coulomb interaction plays a role as well in the onsite (short range) Coulomb interaction. The charge order has been recognized as one of the ground states in a highly correlated electron system. The extended Hubbard model explains that the superconductivity, antiferromagnetic order, and charge order segregate each other [12]. On the other hand, the coexistence of the magnetic (spin) and charge order has been rarely discussed.

A stripe structure due to the charge order was observed in the antiferromagnetic phase of Fe_{1+x}Te by STM [13–18]. The STM image was explained by the charge disproportionation in Fe sites [13,14] with an

antiferromagnetic order. It strongly suggests that both the antiferromagnetic and charge order cooperate and that the strength of U and V is thought to be comparable. We are interested in how to cooperate between the spin and charge order. FeX ($X = \text{S}, \text{Se}, \text{Te}$) [19] has the simplest crystal structure among the iron-based superconductors. It has a layered structure without a blocking layer in contrast to other iron-based superconductors [1,2,20,21]. FeX is suitable to study intrinsic electronic properties since it has only a single conducting layer. Fe_{1+x}Te contains excess iron depending on the synthesis temperature. Its electronic properties depend on the amount of excess iron x [22–24]. The strength of the antiferromagnetic order can be controlled by changing x . In this study, we focused on $\text{Fe}_{1.10}\text{Te}$ of which the Neel temperature T_N is higher.

Experimentally, the charge order has been studied mainly by NMR [25,26], infrared, and Raman spectroscopy [10,27] in organic conductors. The dielectric response has also been measured in organic conductors [28]. The charge order transition was clearly observed in the temperature dependence of the dielectric permittivity revealing that the dielectric response is useful to study the charge fluctuation. Dielectric permittivity was measured in Fe_{1+x}Te at room temperature [29]. The antiferromagnetic state of Fe_{1+x}Te has not been studied by the dielectric response.

STM, which can observe the charge distribution in real space with

Abbreviations: STM, Scanning tunneling microscopy.

* Corresponding author.

E-mail address: ichimura@eng.hokudai.ac.jp (K. Ichimura).

¹ Present address: Department of Sciences and Informatics, Muroran Institute of Technology, Muroran 050–8585, Japan.

<https://doi.org/10.1016/j.ssc.2023.115262>

Received 22 April 2023; Received in revised form 10 June 2023; Accepted 19 June 2023

Available online 21 June 2023

0038-1098/© 2023 Elsevier Ltd. All rights reserved.

atomic resolution, is also a powerful tool to study the charge order. The charge order was directly imaged in high- T_C cuprates [9,30]. The charge disproportionation in the metallic phase was studied in organic conductors [31,32].

We performed STM and dielectric measurement to elucidate the charge fluctuation in the antiferromagnetic order on $\text{Fe}_{1.10}\text{Te}$. In this manuscript, we report the results of the STM and dielectric response and discuss the cooperation of the charge and spin fluctuation.

2. Experimental

Single crystalline samples of $\text{Fe}_{1.10}\text{Te}$ were grown by chemical vapor transport using iodine as the transport agent. Fe and Te were placed in an evacuated quartz tube with a small amount of iodine. The quartz tube was heated at 600 °C for one week. The magnetic susceptibility was measured with a SQUID magnetometer for several flakes of single crystals, which were wrapped by Al foil, while applying a magnetic field of 1 T. The DC resistance and complex impedance were measured in a four-probe configuration with applying current or voltage in the a -direction. An LCR meter HP4274A was used for the complex impedance measurement. A single crystalline sample with dimensions of about $1 \times 1 \times 0.1 \text{ mm}^3$ was used for transport measurements. In the DC measurement, the voltage was measured with a constant current of 0.1–0.5 mA. The complex impedance was measured by applying an AC voltage with an amplitude of 0.06 V for various frequencies of 0.1 k–100 kHz. A low temperature ultrahigh vacuum STM (UNISOKU) was used for STM study. The sample for STM measurement was cleaved at $T = 80 \text{ K}$ in an ultrahigh vacuum. The topographic images were taken at $T = 8.3 \text{ K}$.

The chemical composition of the present sample was determined as $\text{Fe}_{1.10 \pm 0.01}\text{Te}$ by the inductively coupled plasma-atomic emission spectroscopy (ICP-AES) using an ICP-9000 (SHIMADZU). The lattice parameters were determined as $a = b = 3.828 \text{ \AA}$ and $c = 6.287 \text{ \AA}$ by X-ray diffraction for single crystals at room temperature. The chemical composition and lattice parameters were consistent with those of previous reports [23,24].

3. Results and discussion

Fig. 1 shows the temperature dependence of the magnetic susceptibility χ of $\text{Fe}_{1.10}\text{Te}$ applying the magnetic field of 1 T. From $T = 300 \text{ K}$ to 70 K, χ increased linearly with the decrease in temperature. χ decreased sharply at $T = 70 \text{ K}$ and increased down to $T = 4 \text{ K}$. The rapid drop corresponded to the antiferromagnetic transition. The Neel temperature T_N of the sample was estimated at $T_N = 70 \text{ K}$, which is consistent with the reported T_N of $\text{Fe}_{1.11}\text{Te}$ [24].

Fig. 2(a) shows the topographic STM image of $\text{Fe}_{1.10}\text{Te}$ with the bias voltage of 1 V and the tunneling current of 0.05 nA at $T = 8.3 \text{ K}$. Periodic bright spots were observed as a square lattice. The spots corresponded to

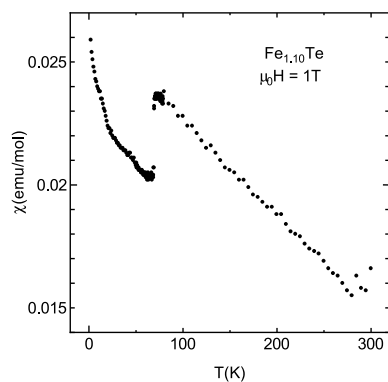


Fig. 1. Temperature dependence of the magnetic susceptibility χ , applying magnetic fields of 1 T.

the Te sites at the outermost surface. The observed square lattice, of which the lattice spacing was 3.8 Å, was consistent with the crystal structure of Fe_{1+x}Te [23,24]. There were a considerable number of obscure spots neighboring the Te sites. The spots were considered to be excess iron sites [33]. The concentration of obscure spots, which was estimated at about 0.09 per Te site, was almost consistent with the chemical composition of the present sample $\text{Fe}_{1.10}\text{Te}$. The Fe sites were located at the midpoint between the nearest neighboring Te sites. Fig. 2 (b) shows the line profiles along the red and green line, which are parallel to the a or b direction, in Fig. 2(a). The red and green line profiles show the Te and Fe sites, respectively. The red line profile shows a periodicity of 3.8 Å, which was consistent with the lattice parameters of $a = b = 3.828 \text{ \AA}$. The green line profile, which corresponds to the Fe site, shows the lattice periodicity as the red one. This result means that each Fe site was equivalent in contrast to the STM result in Fe_{1+x}Te [13–18], which had two-fold lattice periodicity at the Fe site originating from the charge order. A definite charge modulation was not found in the $\text{Fe}_{1.10}\text{Te}$ by the present STM measurement.

In order to study the charge fluctuation from another point of view, we performed DC resistance and AC impedance measurements. Fig. 3 shows the temperature dependence of the DC resistance for various currents $I = 0.1, 0.2, 0.3, 0.4,$ and 0.5 mA . Resistance curves were essentially the same irrespective of the current. In the whole temperature range, plots for different currents overlapped suggesting ohmic behavior. It assures that DC resistance was measured without the Joule heating. Above $T > 70 \text{ K}$, the resistance slightly increased as the temperature decreased. The resistance decreased rapidly at $T = 70 \text{ K}$, which corresponded to T_N . Below T_N , the DC resistance decreased as T decreased. The temperature dependence is similar to previous report for $\text{Fe}_{1.11}\text{Te}$ [24].

In AC measurements, the temperature dependence of the real part of the impedance was essentially the same as that of DC resistance. It assures that AC impedance was measured without the Joule heating. Fig. 4 shows the temperature dependence of the normalized dielectric permittivity of $\text{Fe}_{1.10}\text{Te}$ measured at various frequencies from 1 k to 10 kHz. Since the thickness of the sample was too thin to measure accurately, we do not refer to the absolute value of dielectric permittivity. Here, we define the normalized dielectric permittivity ϵ_N , which is normalized by at $T = 70 \text{ K}$ for $f = 10 \text{ kHz}$. Each color corresponds to the frequency from 1 k to 10 kHz. Above T_N , ϵ_N was almost constantly exhibiting metallic behavior. An anomaly was found at $T_N = 70 \text{ K}$. At T_N , ϵ_N jumped and increased continuously as T decreased below T_N . The temperature dependence below T_N is reminiscent of the paraelectric state.

In order to discuss the paraelectric behavior, we plotted the inverse of ϵ_N . Fig. 5 shows the temperature dependence of $1/\epsilon_N$. We found the linear temperature dependence of $1/\epsilon_N$ changing the slope at about $T = 50 \text{ K}$. As shown in Fig. 5, $1/\epsilon_N$ depended linearly on the temperature at $T < 50 \text{ K}$. Each line in Fig. 5 represents the T -linear curve obtained by the least-squares fitting. The linear behavior of $1/\epsilon_N$ corresponded to the Curie law $\epsilon_N(T) = C/T$, indicating the paraelectric state where C is proportional to the Curie constant. Therefore, the anomaly at T_N corresponded to the metal-paraelectric transition. The paraelectric state appeared with the antiferromagnetic order. This suggests some relation between the spin and charge degrees of freedom. Paraelectricity is regarded as a dynamical charge disproportionation. On the other hand, STM can detect a static charger disproportionation *i.e.* the charge ordered state. The observed paraelectric response was not inconsistent with the STM result, in which a clear charge modulation was not observed in contrast to the case of $\text{Fe}_{1.14}\text{Te}$ [13,14]. The charge order transition has been observed as the paraelectric-ferroelectric transition by the dielectric response in organic conductors, which are a typical material exhibiting the charge order [28]. It is noteworthy that the observed $\epsilon_N(T)$ is similar to that above the charge order transition temperature T_{CO} for organic conductors.

The frequency dependence of C , which is proportional to the Curie

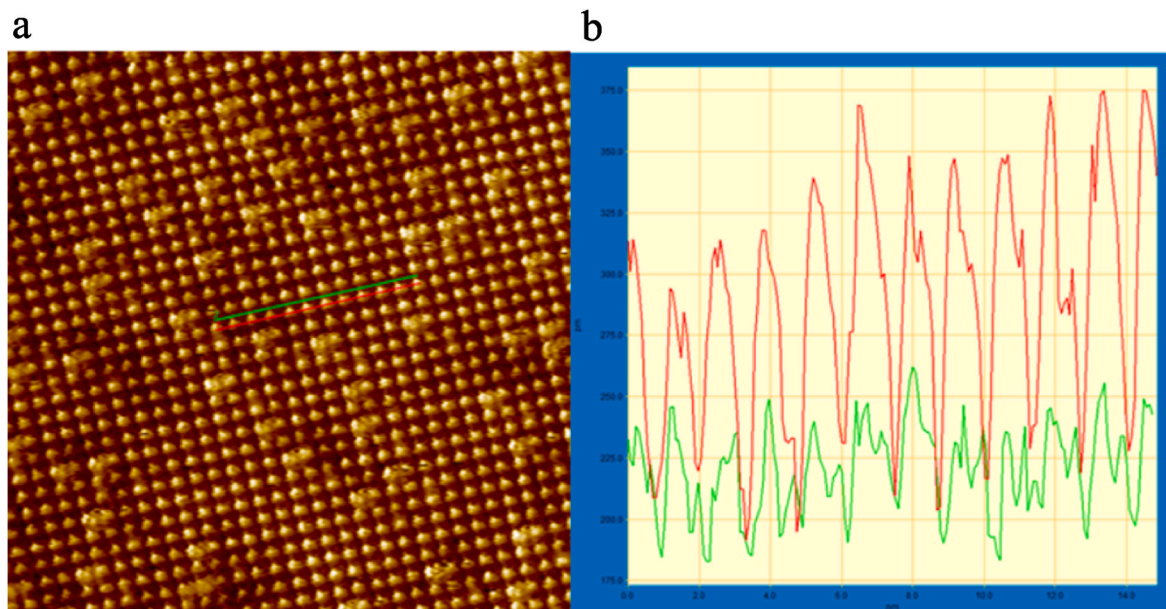


Fig. 2. (A) STM topographic image of the a - b plane at $T = 8.3$ K. (b) Line profiles along the red and green lines in (a). (For interpretation of the references to color in this figure legend, the reader is referred to the Web version of this article.)

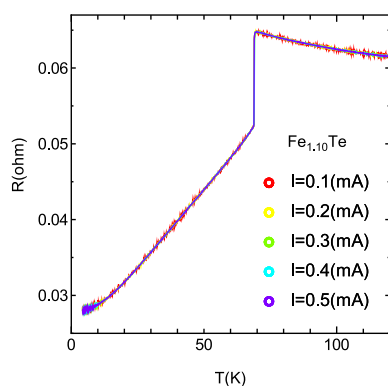


Fig. 3. Temperature dependence of DC resistivity for current $I = 0.1, 0.2, 0.3, 0.4,$ and 0.5 mA.

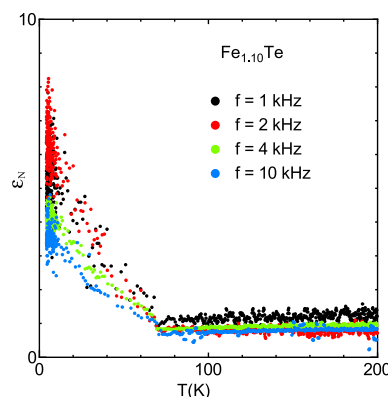


Fig. 4. Temperature dependence of the normalized dielectric permittivity ϵ_N for $f = 1$ k, 2 k, 4 k and 10 kHz.

constant, also suggests a precursor of the charge order. As shown in Fig. 5, the slope of $1/\epsilon_N(T)$ depended on the frequency. The slope increased with the increase in frequency. Correspondingly, C' decreased with the increase in frequency. Similar behavior has been reported in

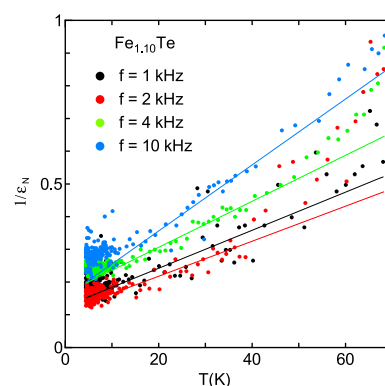


Fig. 5. Temperature dependence of $1/\epsilon_N$ for $f = 1$ k, 2 k, 4 k, and 10 kHz. The solid lines represent the Curie law.

organic conductors $(\text{TMTTF})_2\text{AsF}_6$ [34] and $(\text{TMTTF})_2\text{SbF}_6$ [35], which are typical charge order materials. These materials undergo the paraelectric-ferroelectric transition at T_{CO} . Above T_{CO} , $\epsilon(T)$ followed the Curie law. In addition, the Curie constant decreased with the increase in frequency. The reason is still unclear. However, such a frequency-dependent Curie constant definitely characterizes the charge order transition. Therefore, we think that the observed paraelectric state in $\text{Fe}_{1.10}\text{Te}$ is a precursor of the charge order.

The frequency dependent $\epsilon(T)$ was also reported in the organic conductor κ -(BEDT-TTF) $_2\text{Cu}_2(\text{CN})_3$ [36], which is a dimer type organic conductor with a half-filled conduction band. Paraelectric $\epsilon(T)$ showed a frequency dependence regarded as a relaxor. In this case, T_{max} , where $\epsilon(T)$ showed its maximum, varied depending on the frequency with the same Curie constant. On the other hand, the Curie constant depended on frequency in the present case of $\text{Fe}_{1.10}\text{Te}$. Moreover, the dielectric response appeared without magnetic order in κ -(BEDT-TTF) $_2\text{Cu}_2(\text{CN})_3$ in contrast to the case of $\text{Fe}_{1.10}\text{Te}$ where the Curie-like dielectric response appeared in the antiferromagnetic phase. In κ -(BEDT-TTF) $_2\text{Cu}_2(\text{CN})_3$, the intradimer Coulomb repulsion was substantially large. The charge disproportionation occurred within the dimer with $s = 1/2$ spin per dimer. As a result, both spin and charge correlations exist. Such a situation is partially similar to the case of $\text{Fe}_{1.10}\text{Te}$. However, the

present result of the frequency-dependent Curie constant differs from the relaxor like behavior in κ -(BEDT-TTF)₂Cu₂(CN)₃. Another model is needed to explain the frequency-dependent Curie constant in Fe_{1.10}Te.

The twinned microstructure was reported in the antiferromagnetic phase by STM [16,17]. The twinned microstructure might be a possible origin of the observed paraelectric behavior. If there is some relationship between charge and spin degrees of freedom, the antiferromagnetic state with twinned microstructure might bring about the paraelectric fluctuation rather than ferroelectric order.

The present result indicates that the charge fluctuation exists in the antiferromagnetic state. It is of great interest that both the spin and charge degrees of freedom play an important role. In general, the magnetic (spin) and charge order originate from the onsite (short range) and offsite (long range) Coulomb interaction, respectively. The charge order is understood to gain the long range Coulomb interaction similar to the Wigner crystal [37]. These highly correlated electron systems are described by the extended Hubbard model [11,12], where both the onsite and offsite Coulomb interactions are taken into account, as well as the transfer energy. The coexistence of the antiferromagnetic and charge order is discussed in a one-dimensional system [11]. On the other hand, either the spin or charge order has been observed in a two-dimensional system. The present and previous results [13,14] in Fe_{1+x}Te suggest that both spin and charge fluctuations play a role in the two-dimensional system. Some mechanism is needed to explain our finding of the coexistence of the antiferromagnetic and charge fluctuation in Fe_{1+x}Te.

4. Conclusions

Fe_{1.10}Te was studied by STM and dielectric response to elucidate the charge fluctuation in the antiferromagnetic state. The temperature dependence of the magnetic susceptibility clearly showed the antiferromagnetic transition at $T_N = 70$ K. STM images taken below T_N showed no clear charge modulation in contrast to the previous study on Fe_{1.14}Te. The temperature dependence of the dielectric permittivity showed a clear metal-paraelectric transition at T_N . Below T_N , the dielectric permittivity followed the Curie law, indicating the charge fluctuation with the antiferromagnetic order. We conclude that charges fluctuate dynamically in the antiferromagnetic state. Both the charge and spin degrees of freedom cooperate in Fe_{1.10}Te.

Author statement

Kazuoki Yokoi: Conceptualization, Methodology, Sample preparation, Writing-Original draft preparation, Investigation, Data curation, Issei Miyazaki: Conceptualization, Methodology, Sample preparation, Investigation, Data curation, Koichi Ichimura: Conceptualization, Methodology, Validation, Investigation, Writing-Reviewing and Editing, Supervision, Project administration, Funding acquisition, Satoshi Tanda: Investigation, Noriaki Matsunaga: Methodology, Investigation, Tohru Kurosawa: Methodology, Investigation, Data curation, Migaku Oda: Investigation.

Declaration of competing interest

The authors declare that they have no known competing financial interests or personal relationships that could have appeared to influence the work reported in this paper.

Data availability

The data that has been used is confidential.

Acknowledgments

The authors are grateful to Dr. M. Sakoda for the valuable discussion. This work was supported by JSPS KAKENHI Grant Number JP17K05526 and Iketani Science and Technology Foundation.

References

- [1] Y. Kamihara, H. Hiramatsu, M. Hirano, R. Kawamura, H. Yanagi, T. Kamiya, H. Hosono, *J. Am. Chem. Soc.* 128 (2006), 10012.
- [2] Y. Kamihara, T. Watanabe, M. Hirano, H. Hosono, *J. Am. Chem. Soc.* 130 (2008) 3296.
- [3] T. Ishiguro, K. Yamaji, G. Saito, *Organic Superconductors*, second ed., Springer-Verlag, Berlin, Germany, 1998.
- [4] P. Dai, *Rev. Mod. Phys.* 87 (2015) 855.
- [5] J. Hubbard, *Proc. Roy. Soc. A* 276 (1963) 238.
- [6] J. Hubbard, *Proc. Roy. Soc. A* 277 (1964) 237.
- [7] J. Hubbard, *Proc. Roy. Soc. A* 281 (1964) 401.
- [8] J.M. Tranquada, B.J. Sternlieb, J.D. Axe, Y. Nakamura, S. Uchida, *Nature* 375 (1995) 561.
- [9] C. Howald, H. Eisaki, N. Kaneko, M. Greven, A. Kapitulnik, *Phys. Rev. B* 67 (2003), 014533.
- [10] T. Takahashi, Y. Nogami, K. Yakushi, *J. Phys. Soc. Jpn.* 75 (2006), 051008.
- [11] H. Seo, H. Fukuyama, *J. Phys. Soc. Jpn.* 66 (1997) 1249.
- [12] H. Seo, J. Merino, H. Yoshioka, M. Ogata, *J. Phys. Soc. Jpn.* 75 (2006), 051009.
- [13] Y. Kawashima, K. Ichimura, J. Ishioka, T. Kurosawa, M. Oda, K. Yamaya, S. Tanda, *Solid State Commun.* 167 (2013) 10.
- [14] Y. Kawashima, K. Ichimura, J. Ishioka, T. Kurosawa, M. Oda, K. Yamaya, S. Tanda, *Physica B* 407 (2012) 1796.
- [15] W. Li, W.G. Yin, L. Wang, K. He, X. Ma, Q.K. Xue, X. Chen, *Phys. Rev. B* 93 (2016), 041101.
- [16] J. Warmuth, M. Bremholm, P. Hofmann, J. Wiebe, R. Wiesendanger, *NPJ Quantum Mater* 21 (2018) 3.
- [17] S. Rößler, C. Koz, Z. Wang, Y. Skourski, M. Doerr, D. Kasinathan, H. Rosner, M. Schmidt, U. Schwarz, U.K. Rößler, S. Wirth, *Proc. Natl. Acad. Sci. U.S.A.* 116 (2019), 16697.
- [18] C. Trainer, C.M. Yim, C. Heil, F. Giustino, D. Croitor, V. Tsurkan, A. Loidl, E. E. Rodriguez, C. Stock, P. Wahl, *Sci. Adv.* 5 (2019) 3478.
- [19] F.C. Hsu, J.Y. Luo, K.W. Yeh, T.K. Chen, T.W. Huang, P.M. Wu, Y.C. Lee, Y. L. Huang, Y.Y. Chu, D.C. Yan, M.K. Wu, *Proc. Natl. Acad. Sci. U.S.A.* 105 (2008), 14262.
- [20] M. Rotter, M. Tegel, D. Johrendt, *Phys. Rev. Lett.* 101 (2008), 107006.
- [21] J.H. Tapp, Z. Tang, B. Lv, K. Sasmal, B. Lorenz, P.C.W. Chu, A.M. Guloy, *Phys. Rev. B* 78 (2008), 060505.
- [22] W. Bao, Y. Qiu, Q. Huang, M.A. Green, P. Zajdel, M.R. Fitzsimmons, M. Zhernenkov, S. Chang, M. Fang, B. Qian, E.K. Vehstedt, J. Yang, H.M. Pham, L. Spinu, Z.Q. Mao, *Phys. Rev. Lett.* 102 (2009), 247001.
- [23] E.E. Rodriguez, C. Stock, P. Zajdel, K.L. Krycka, C.F. Majkrzak, P. Zavalij, M. A. Green, *Phys. Rev. B* 84 (2011), 064403.
- [24] C. Koz, S. Rößler, A.A. Tsirlin, S. Wirth, U. Schwarz, *Phys. Rev. B* 88 (2013), 094509.
- [25] K. Hiraki, K. Kanoda, *Phys. Rev. Lett.* 80 (1998) 4737.
- [26] K. Kanoda, *J. Phys. Soc. Jpn.* 75 (2006), 051007.
- [27] K. Yamamoto, K. Yakushi, K. Miyagawa, K. Kanoda, A. Kawamoto, *Phys. Rev. B* 65 (2002), 085110.
- [28] F. Nad, P. Monceau, *J. Phys. Soc. Jpn.* 75 (2006), 051005.
- [29] E.H.H. Lim, J.Y.C. Liew, M.M.A. Kechik, S.A. Halim, K.B. Tan, O.J. Lee, S.K. Chen, *J. Supercond. Nov. Magnetism* 30 (2017) 2915.
- [30] N. Momono, A. Hashimoto, Y. Kobatake, M. Oda, M. Ido, *J. Phys. Soc. Jpn.* 74 (2005) 2400.
- [31] K. Katono, T. Taniguchi, K. Ichimura, Y. Kawashima, S. Tanda, K. Yamamoto, *Phys. Rev. B* 91 (2015), 125110.
- [32] K. Katono, T. Taniguchi, K. Ichimura, Y. Kawashima, K. Yamaya, S. Tanda, *Physica B* 460 (2015) 64.
- [33] T. Kato, Y. Mizuguchi, H. Nakamura, T. Machida, H. Sakata, Y. Takano, *Phys. Rev. B* 80 (2009), 18507.
- [34] F. Nad, P. Monceau, C. Carcel, J.M. Fabre, *J. Phys. Condens. Matter* 13 (2001) L717.
- [35] M. Nagasawa, F. Nad, P. Monceau, J.M. Fabre, *Solid State Commun.* 136 (2005) 262.
- [36] M. Abdel-Jawad, I. Terasaki, T. Sasaki, N. Yoneyama, Y. Uesu, C. Hotta, *Phys. Rev. B* 82 (2010), 125119.
- [37] E. Wigner, *Phys. Rev.* 46 (1934) 1002.